*IOSR Journal of Mechanical and Civil Engineering (IOSR-JMCE)*
*e-ISSN: 2278-1684,p-ISSN: 2320-334X, Volume 10, Issue 4 (Nov. - Dec. 2013), PP 50-59*
*www.iosrjournals.org*

# Study of the Tribological behavior of as cast Al-4.2%Cu-$Al_2O_3$ composite

[1]S. Srivastava, [2]P. K. Singh, [2]S. K. Singh, [1]Somya Yadav, [1]Yogesh Srivastav
*[1]Materials Science & Metallurgical Engineering*
*[1]Maulana Azad National Institute of Technology, Bhopal, M.P. (India)*
*[2]University of Technology, Barkatullah University, Bhopal, M.P. (India)*

***Abstract:*** *The research work is carried out on the study of tribological property of aluminium based metal matrix composite material, which is fabricated by using sol-gel technique. The composite material is prepared through liquid metallurgy method by using varying percentage of Alumina and aluminium and fixed percentage of copper 4.2%. Test sample billet is fabricated through casting method and has been examined the different mechanical behaviour such as* Vickers Hardness Number, *Ultimate Tensile Strength, 0.2% Proof Stress, etc.*
*From the study, it has been observed that with increase in the alumina content in matrix the ductility of composite show a contrary effect. The Pin-On-Disc test is used to evaluate the tribological property wear for composite material and it is observered that tendency of wear rate has improved. The weight losses of the specimen are measured and wear and friction characteristics are calculated with respect to time. Depth of wear track, sliding speed, bearing load friction coefficient and wear volume have been shown large sensitivity to the applied normal load and the testing time (or sliding distance). The XRD and SEM analysis are used to analyse the wear debris and track; and silent conclusion has been drawn.*
***Key words:*** *Tribological, composite, wear, pin-on-disc, friction, XRD, SEM.*

## I. Introduction

Aluminum matrix composites (AMCs) refer to the class of light weight high performance aluminum centric material systems. The properties of AMCs can be tailored to the demands of different industrial applications by suitable combinations of matrix, reinforcement and processing route. Presently several grades of AMCs are manufactured by different routes. Three decades of intensive research have provided a wealth of new scientific knowledge on the intrinsic and extrinsic effects of ceramic reinforcement vis-a-vis physical, mechanical, thermo-mechanical and tribological properties of AMCs. In the last few years, AMCs have been utilized in high-tech structural and functional applications including aerospace, defence, automotive, and thermal management areas, as well as in sports and recreation. It is interesting to note that research on particle-reinforced cast AMCs took root in India during the 70's, attained industrial maturity in the developed world and is currently in the process of joining the mainstream of materials. This work represents an overview of AMC material systems on aspects relating to processing, microstructure, properties and applications.

## II. Experimental investigation

**Selection of materials**

The material used in this work was commercially available 99·5% pure aluminum with a composition given in table 1. Commercially pure aluminium is the product of the electrolytic cell process. In this experiment, the composite of Al-Cu was prepared from commercial pure aluminum with the appropriate addition of 99.99% small chips of pure tin-metal. Table 2 shows the physical and mechanical properties of pure aluminum.

| Element wt.% | Si | Fe | Ti | V | Cu | Mn | Al | Others |
|---|---|---|---|---|---|---|---|---|
| | 0.063 | 0·36 | 0·003 | 0·006 | 0·002 | 0·037 | 99·557 | 0·002 |

**TABLE 1: Chemical composition of the 99·5% pure aluminum.**

| Typical mechanical properties | |
|---|---|
| Density | 2.7g/m$^3$ |
| 0.2% yield strength | 20MPa |
| UTS | 70MPa |
| Elongation | 50% |
| Hardness | 170Hv |

**TABLE 2: Physical and mechanical properties of commercially pure aluminum**

## III. Procedure for preparation

The experimental set-up used for mixing and casting of composites is shown in Fig 16. It comprises of a cylindrical sillimanite crucible of 150 mm diameter and 250mm depth with attachment of four baffles to its sidewalls for proper dispersion of second phase in melt during stirring. The crucible was placed in an electric heated muffle furnace. It was also equipped with a bottom pouring attachment, which could be closed or opened by alumina stopper with a lever system. A steel mould was placed beneath the furnace to cast the molten metal. In the top cover suitable opening was provided to charge materials and insert thermocouples. The temperature of the furnace could be controlled with an accuracy of about $\pm 5^0$C. Metallic bath temperature was measured continuously by chromel /alumel thermocouple. The agitator system could be raised or lowered with the help of the hanger and steel frame structure. After adjusting the mixer in a central position and required height from the bottom of the crucible, the motor was bolted and locked while mixing of melt. Three-blade impeller was used for effective mixing. This design provides very high rates of shear and only axial and radial flow currents are utilized for mixing without any significant vortex formation due to the presence of baffles. The Al-Cu-Alumina composites were prepared by liquid metallurgy methods. The required amounts of commercial (approximately 880-900g) pure aluminum with 65 g of copper were charged into the crucible and aluminum was heated to a temperature $200^0$C above its melting point i.e. $662^0$C. A mechanical stirrer was inserted into the melt, and agitation was started at a speed of 35 $s^{-1}$. Mixing was done for a period of 60 seconds. The emulsion was poured into the chilled cylindrical mould placed beneath the crucible. The same procedure was adopted for different compositions. Cylindrical casting of length 20cm and dia.2cm were obtained.

## IV. Evaluation of as-cast Properties of the Composite

The wet chemical analysis was used to determine the percentage of iron in the bulk .The metallographic specimens were prepared using standard technique and studied under SEM for different feature present. The density of the composite was determined using Archimedes' principle by weighing in water and air. The hardness of the entire composite was measured using a Vickers hardness testing machine. The hardness of the entire composite was measured using a Vickers hardness testing machine. The hardness was measured using Vickers hardness instrument Leitz Welzlar at a load of 5Kg. At least 3 indentations have been taken for each point. Tensile testing of all the Al-alloy-Alumina composite was performed stress along with percentage elongation and reductions in area were computed from the results.

## V. Wear test

Pin-on-disc machine was used for evaluating the wear properties under dry sliding condition. The cylindrical test pin of 8mm diameter and 40mm length were used against a hardened steel disc of 120 mm diameter. Wear tests were conducted with variable applied pressure $3.9 \times 10^{-1}$ MPa and a sliding speed of 0.5 m/s with a constant sliding distance of 10000 meters. Wear test were also conducted with selected varying speeds and sliding distance ranging up to 1000 meters. The initial weight of the specimen was determined in a digital balance with a precision of ± 0.1 mg. The pin was kept pressed against a rotating steel disc of hardness 58 HRC under loaded condition. The frictional traction en-counted by the pin in sliding is measured by a PC based data logging system. On completion of the running through the required sliding distance the specimen pins were cleaned with acetone, dried and their weight were again determined for ascertaining the weight loss. Wear debris were analyzed by XRD.

## VI. Result and Discussion

### 1. Physical investigation

The liquid metallurgy methods were used to synthesize the composite materials with different amount of the alumina content in the matrix. The theoretical density of the composite materials varies from 2.88 g/cc to 2.84 g/cc with alumina content. But the experimental density of the composite materials was found to vary from 2.72 g/cc to 2.70 g/cc along with porosity varies from 5.2 % to 4.9 %. The XRD methods were used to investigate the different phase/element present in the prepared composite materials. Fig 18 shows the XRD pattern of prepared nano $Al_2O_3$ with (012), (104), (110), (133), (024), (116), (018), (214), (119) at an angle of 25.594°, 35.197°, 37.804°, 43.381°, 52.588°, 57.538°, 61.333°, 66.547°, 68.230°. Fig 12(b) shows the XRD pattern of $Al_2O_3$. The XRD scanning from 10°- 80° shows the lines for alumina, 38.86°, for aluminum respectively.

## 2. SEM investigation

In casting a homogeneous single phase liquid is cooled below the liquidus line, it transforms into two liquids, namely aluminum rich and copper rich. The minor 'Cu' rich phase segregates out. If the homogeneous single Al-Cu liquid phase is rapidly cooled, then the minor phase is dispersed uniformly in aluminum rich matrix. The microstructure of the alloys was investigated by using SEM. Fig. 17 shows the microstructure of commercially pure aluminum along with composite in Fig. 18. Here copper and $Al_2O_3$ nanoparticles is distributed in aluminum matrix as a separate phase in form of reticular (network) structure along the edges of aluminum grains with the proper uniform distribution.

## 3. STUDY OF THE MECHANICAL PROPERTIES

| S.No. | Composite | VHN | UTS(MPa) | 0.2%PS(MPa) | % elongation |
|---|---|---|---|---|---|
| 1 | Al-4.2%Cu-1.6%$Al_2O_3$ | 96.2 | 147.3 | 72.9 | 19.3 |
| 2 | Al-4.2%Cu -2.7%$Al_2O_3$ | 99.6 | 152.3 | 79.1 | 18.1 |
| 3 | Al-4.2%Cu -3.4%$Al_2O_3$ | 104 | 158.4 | 83.2 | 17.3 |
| 4 | Al-4.2%Cu -5.6% $Al_2O_3$ | 109 | 165.3 | 87.4 | 16.9 |
| 5 | AL-4.2%CU -8.4% $AL_2O_3$ | 116 | 173.2 | 93.2 | 16.3 |

**TABLE 3: Mechanical properties of the Al-4.2%Cu-3.4%Alumina composite**

The resistance to indentation or scratch is termed as hardness. Among various instruments for measurement of hardness, Brinell's, Rockwell's and Vickers's hardness testers are significant. Theoretically, the rule of mixture of the type $H_c=v_r H_r+v_m H_m$ (suffixes 'c', 'r', and 'm' stand for composite, reinforcement and matrix respectively and *v* and H stand for volume fraction and hardness respectively) is valid for composite materials which helps in approximating the hardness values. Among the variants of reinforcements, the low aspect ratio particle reinforcements are of much significant in imparting the hardness of the material in which they are dispersed. Table 6 shows a comparison of the mechanical properties of Al-Cu/$Al_2O_3$ composite samples produced by the liquid metallurgy methods. Fig. 16 shows the variation of mechanical properties with the Alumina content in the Al-Cu alloys. It is observed that the hardness of the composite materials increases with increasing the alumina content in the matrix. Alumina is a very ductile materials and it is responsible a factor for increasing the hardness of the materials.

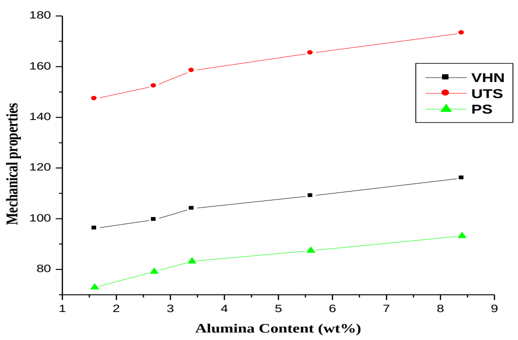


**Fig.1: Variation of hardness with varying alumina content**

The uniform distribution and the nature of the interfacial bonding between alumina particles and matrix have an important relationship on the mechanical properties of a composite material. It has been suggested that alumina particles, being very hard compared to the aluminium matrix, may be treated as load-bearing constituents. With a view to extending their applications to structural components, these materials should have a good combination of strength and ductility. The Al-Cu/Alumina composites with different $Al_2O_3$ content show an decrease in the tensile elongation together with an increase in the ultimate tensile strength of the material, resulting from the better dispersion of the particles. The magnitudes of these decreases are observed to average approximately

18%. A strong bond between the reinforcement and matrix helps in the load transfer from the latter to the former. As a result, fracture takes place in the composite via the reinforcement and not along the interface [1, 2]. Although the alumina is a load bearing constituent, a strong particle/matrix interface helps alumina particles embed themselves into the matrix properly, improving the wear resistance.

## VII. Wear study

### 1. Effect of sliding distance and load

The variation of bulk wear with sliding distance was studied at different combinations of loads and sliding velocities. Almost a linear relationship in bulk wear and sliding distance i.e. steady state wear is observed after an initial running-in period of 500–1000 m in almost all the cases irrespective of load or sliding velocity used. Fig 2 shows the results for a test conducted at 2 kg load and 0.5m/s sliding velocity. In running period, the Al-Cu/Alumina composite shows large wear rates. The relation found here is in accordance with the pattern for most metallic materials derived theoretically as well as observed experimentally [3, 4]. But irrespective of variables used, bulk wear is large with large alumina content in Al-Cu/Alumina composite. The free alumina particles are released from the composite material during dry sliding of mating surfaces form a lubricant film at the interface. Shows the variation of rise in temperature of the test specimen during experiment with sliding distance. The maximum rise in temperature is found in Al-4.2%Cu-8.4%Al2O3 and minimum in Al-4.2%Cu-1.6%Al2O3. This type of the behaviour can be explained on the basis of thermal conductivity. Al-4.2%Cu-1.6%Al2O3 shows high conductivity as Al-4.2%Cu-8.4% $Al_2O_3$. Fig.5 shows the SEM micrographs of wear tracks of Al-Cu/$Al_2O_3$ composites (Al-4.2%Cu-3.4%$Al_2O_3$) for 2 kg applied load and 0.5 m/s sliding velocity at 10,000 m sliding distances. This micrograph was taken at the higher magnification (X6000). This figure is clearly revealed the presence of the oxide layer which might be adhered on the rubbing surface.

### 2. Effect of applied load

The studies conducted to see the effect of applied load on wear rate revealed that wear rate increases continuously with load in a linear manner irrespective of the sliding velocity used as it is evident from Fig.6 for a particular velocity. But in all the cases wear rate first increases with increase in alumina content for all combinations of loads and sliding velocities used in the present investigation and then increases with decrease the alumina content. Corresponding temperature curve shown in, clearly reveal that temperature continuously increases with increase in load but with increase in copper percentage in composite an increase in temperature rise is observed which is indicative of larger heat dissipation capability of copper. the variation of temperature and micro hardness of the test specimen with the variation of load. With increase the load on the test specimen, the composite material bears maximum rise in temperature. The materials at the contacting surface on the pin-on-disc become soften, which is responsible factor for decreasing the micro hardness of the contacting surface.

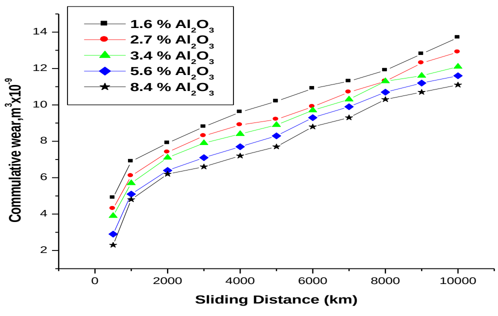


**Fig.2: Variation of bulk wear with sliding distance at 2 kg load and 0.5 m/s sliding velocity for as-cast Al-Cu/Al2O3 composites.**

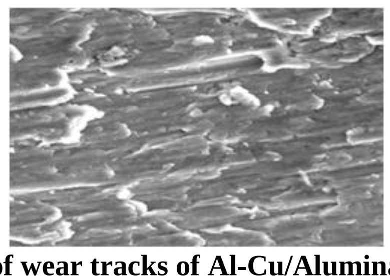

**Fig.3: SEM micrographs of wear tracks of Al-Cu/Alumina composites (Al-4.2%Cu -3.4%Alumina) for 2 kg applied load and 0.5 m/s sliding velocity at 10,000m sliding distances.**

Fig.5 shows the SEM micrographs of wear tracks of Al-Cu/Al2O3 composites (Al-4.2%Cu-3.4%$Al_2O_3$) at the higher magnification for 2 kg applied load and 0.5 m/s sliding velocity at 3000 m sliding distances. The oxides layer with small amount of the alumina particles are adhered on the material surface. Fig 6 (a) and Fig 6 (b) shows the SEM micrographs of wear tracks of Al-Cu/alumina composites (Al-4.2%Cu-3.4% $Al_2O_3$) for 15 kg applied load and 0.5 m/s sliding velocity at 3000 m sliding distances (a) worn surface (b) crack surface. The degree of surface damage (i.e. depth and width of the grooves) depended on the applied load and microstructure of the material. At the higher load, generally metallic failure is observed as shown in Fig 28 (a). For observing the mechanistic phenomena at the higher load, the SEM micrograph was taken at the higher magnification, as shown in Fig 6 (b). While studying the wear tracks at different loads for a particular velocity (from 2 to 15 Kg) the operating modes changes from oxidative-to oxidative and metallic to metallic as load applied is increased and wear track observes broken oxide film, deep grooves and delaminating of surface as evident from Fig 6 (b). In this SEM micrograph some small crack was found at the oxide surface. With increase the load, the produce cracks within the material by sliding action easily propagate and the form oxidative film at lower load are ruptured as shown in Fig 6 (b) at 15 Kg load and 0.7m/sec sliding velocity

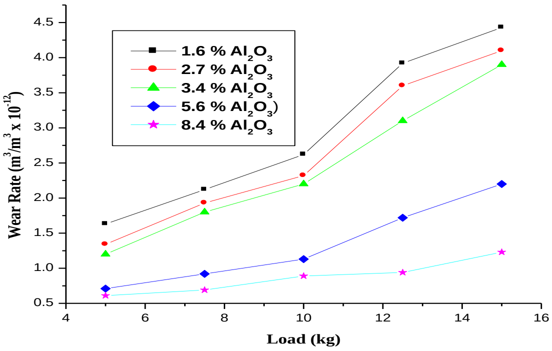


**Fig.4: Variation of wear rate with load at 0.5 m/s sliding velocity and running distance 3000 m for as-cast Al-Cu/ $Al_2O_3$ composites**

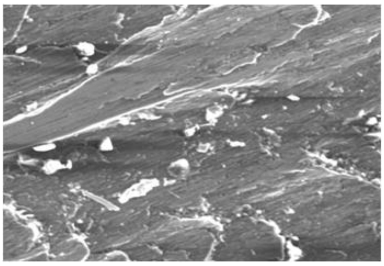

**Fig.5: SEM micrographs of wear tracks of Al-Cu/Alumina composites (Al-4.2%Cu-3.4% $Al_2O_3$) for 2 kg applied load and 0.5 m/s sliding velocity at 3000 m sliding distances.**

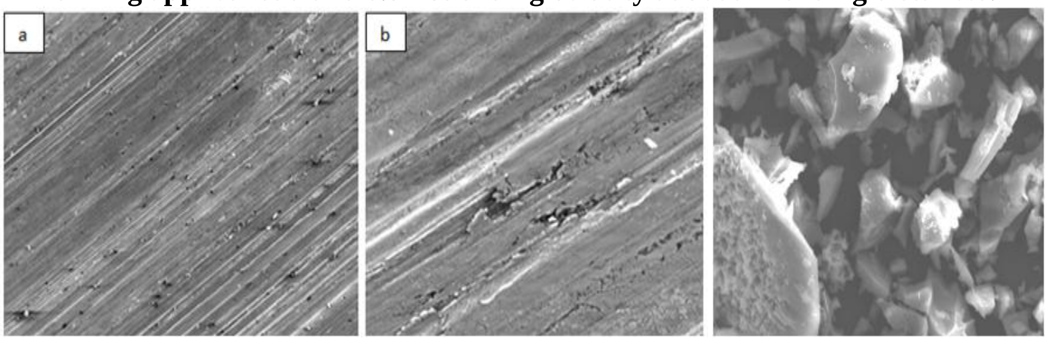


**Fig.6: SEM micrographs of wear tracks of Al-Cu/ $Al_2O_3$composites (Al-4.2%Cu-3.4% $Al_2O_3$) for 15 kg applied load and 0.5 m/s sliding velocity at 3000 m sliding distances (a) worn surface (b) crack surface (c) Al2O3**

## 3. Study of the sliding velocity

The role of alumina in sliding contact is provided by layered-lattice structure. The bonds between the parallel layers are relatively strong. The adsorbed water vapor and other gases from environment onto the crystalline edges weaken the interlayer bonding forces. It results in easy shear and transfer of the crystalline platelets on the mating surfaces. Fig 7 shows the variation of wear rate with sliding velocity at 2 kg load, 3000m running distance. Like all other aluminium alloys/ composites, Al-Cu/ $Al_2O_3$ composites also show an initial decrease in wear rate followed by a sharp increase in wear rate after attaining minima with increase of sliding velocity for all composites at different loads. But in all the cases wear rate decreases with increase in alumina content for (say up to 3.4 % $Al_2O_3$ in the matrix) all combinations of loads and sliding velocities used. While that wear rate again decrease with increase the alumina content in the matrix.

Further, variation of wear rate and hardness of worn wear track surface is shown in Fig 8. It clearly shows highest hardness at minima in wear rate, which is clearly indicative of the presence of hard oxide particles. With increase in sliding velocity, an oxides particle is removed from the mating surface, due to decrease the hardness of the composite materials and hence increases the wear rate. For temperature increase with sliding velocity follows the same trend as observed in the case of variation of temperature with applied load. Higher velocity gives higher amount of wear loss due to fast rubbing of the contacting surface. Therefore maximum rise in temperature in the test specimen at the contacting surface occurs. The SEM observations of the wear tracks at 2.0 Kg load for different sliding velocities are shown in Fig.9 (a–b) and 10(a–c). In Fig.9 (a-b) shows the SEM observation at the lower and the higher velocity and Fig 10(a-c) show SEM result at the optimized velocity. SEM micrograph of the wear track in Fig 9(a) was mainly comprised of oxide particles and the wear track surface is seen to have more pronounced layer of oxide particles adhered at the surface of the materials. But at the higher velocity, metallic particles come out during wear processes and wear track is seen clear and smooth as shown in Fig.9 (b).

The minima in the wear rate was found at 1.22 m/sec. Fig. 16 show SEM micrographs of wear tracks of Al-Cu/ $Al_2O_3$ composites (Al-4.2%Cu-3.4% $Al_2O_3$) for 2 kg applied load and 1.22 m/s sliding velocity at 3000 m sliding distances (a) worn surface (b) crack observation (c) observation of the oxide layer. Wear rate continuously increases with increase the sliding velocity due to the formation of thin film of oxide layers along with metallic layer at the mating surface as shown in Fig 10 (a). This is confirmed from the SEM observation of the wear track taken at the higher magnification as shown in Fig.10(b).

The oxide layer of the respective metals adhered on the mating surface is clearly visible in this micrograph. The failure of the materials from the wear process is due to formation and propagation of the crack within the materials as shown in Fig 10(c). The cracks are formed at the adjacent surface of the materials. An examination of the three micrographs shows the formation of severe patches and grooves resulting from plastic deformation of the aluminium alumina composite and relatively small groves and mild patches on 3.4 wt % alumina composite. This reduction in severity of the worn surface of the composite material is due to the formation of a $Al_2O_3$ lubricating film which prevents the direct contact of the specimen with the rotating steel disc surface. This formation of the lubricating layer at the sliding surface becomes thicker with more alumina as the addition of $Al_2O_3$ content to the base alloy increases and it is responsible for playing an effective role for keeping the wear behaviour of the composite low.

## 4. Study of the surface particles and its mechanistic approach

Figure 11 (a-b) shows the SEM micrograph of wear debris for 2 kg applied load and 1.22 m/s sliding velocity at 3000 m sliding distances (a) collecting particles (b) examination of the alumina particles. This observation has been also confirmed by XRD observation as shown in Fig.12. Debris in all figures was mainly comprised of oxide particles of aluminum and tin. But it also contained some small amount of alumina as shown in Figure 11(b). In the XRD observation, the aluminum oxide, tin and its oxides (from EDAX observation) and alumina are found as the main peak. Tin and lead are weak and ductile and hence they decrease the strength property of aluminium alloys under study. Further, Cu/ $Al_2O_3$, being a ductile material, deforms in preference to the stronger matrix. This reduces the stress concentration in the matrix and makes it more deformable. It is also found that the alloys containing tin have slightly more strength and hardness but low ductility values compared to the alloys containing lead.

Al wear particles on the worn surfaces are laminated by the pin on the contact area, forming plough. Because wear particles contain some aluminum oxide, Zhou et al believed that the oxidation wear was the main wear mechanism of composites [5]. However, according to the SEM observation of worn surfaces of the composite and the study of delamination theory of wear, it can be concluded that the delamination wear could be the main wear mechanism. Dislocations at the mating surface, subsurface crack and void are induced due to the repeated plastic deformation between the test pin and disc. The cracks extend later and cause break and split of the hardened surface layer by shear deformation mechanism [6-10].

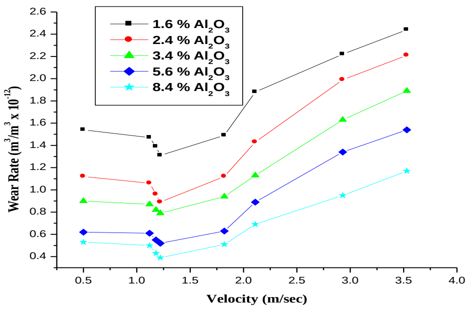


**Fig.7: Variation of wear rate with sliding velocity at 2 kg load for Al-Cu/ $Al_2O_3$ composites.**

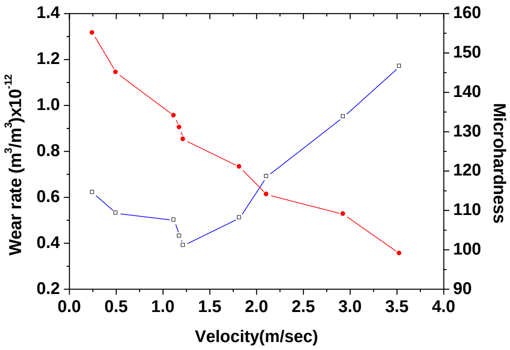


**Fig.8: Variation of micro-hardness and wear rate of worn surface with sliding velocity at 2 kg load.**

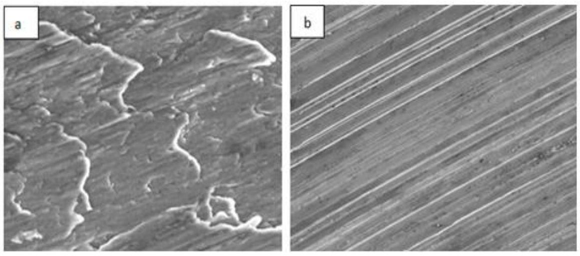


**Fig.9: SEM micrographs of wear tracks of Al-Cu/ $Al_2O_3$ composites (Al-4.2%Cu-3.4% $Al_2O_3$) for 2 kg applied load and 0.5 m/s sliding velocity at 3000 m sliding distances (a) worn surface at 0.25m/sec (b) worn surface at 3.53m/sec**

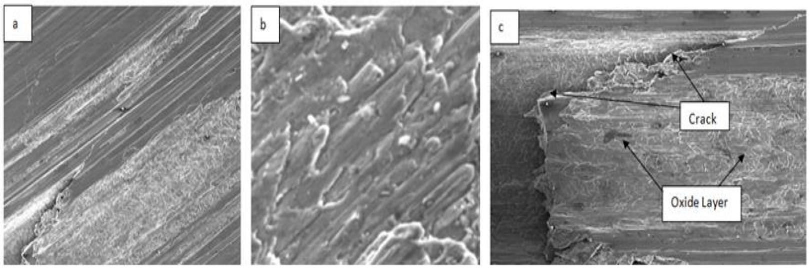


**Fig.10: SEM micrographs of wear tracks of Al-Cu/ $Al_2O_3$ composites (Al-4.2%Cu-3.4% $Al_2O_3$) for 2 kg applied load and 1.22 m/s sliding velocity at 3000 m sliding distances (a) and (b) worn surface (c) observation of the oxide layer**

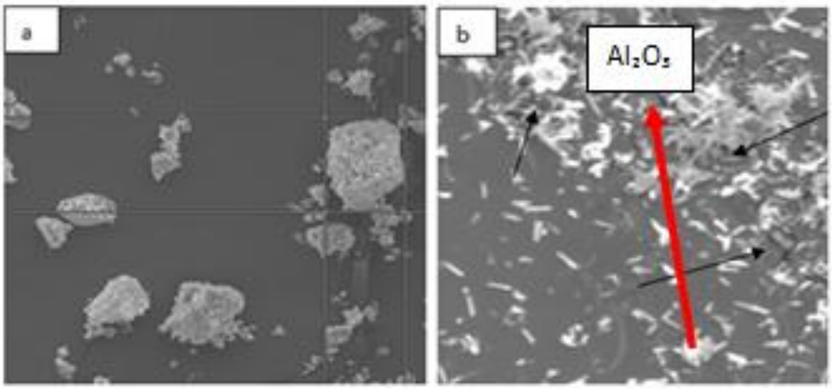


**Fig.11: SEM micrographs of wear debris of Al-Cu/ $Al_2O_3$ composites (Al-4.2%Cu-3.4% $Al_2O_3$) for 2 kg applied load and 1.22 m/s sliding velocity at 3000 m sliding distances (a) collecting particles (b) examination of the alumina particles.**

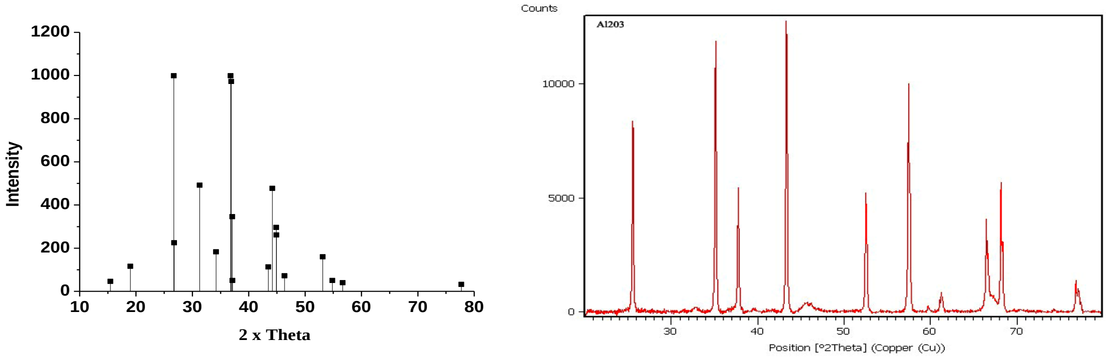


**Fig.12: (a) XRD of the wear debris. b) XRD of $Al_2O_3$.**

## 5. Friction studies

The characterization of friction behaviour of Al-Cu/Alumina base composite with sliding at the specific load (i.e. 10N) is illustrated in Fig 13. The Figure show is graphically representation of the results obtained from the friction experiment at a fixed load and sliding velocity. It is evident from the Fig.13 the friction coefficient drastically increases during the running in period. During the steady state period the friction coefficient is being stabilized. In dry sliding, the reason for increasing the wear rate and the coefficient of friction of Al-Cu/ $Al_2O_3$ composite as compared with the base alloy is the presence of alumina layer at the sliding surface which acts as the best solid lubricant. The friction behaviour also varies with applied load. The average value of the friction coefficient at normal load is shown in Fig.14. In accordance with the figure the decrease of the friction coefficient corresponds to increase the normal load. The increase rate is especially evident for load change from 10 to 50 kg. On increasing the applied load, lubricating condition of the alumina improves; the alloy composition starts to play its role in determining the running ability of the test under friction. Fig.15 shows the variation of coefficient of friction with wt % of alumina content in the matrix. The friction coefficient of the test materials increases with increase the alumina content in the matrix. With increasing the alumina content, the thickness of the lubricating film and the amount the alumina in the lubricating film decreases. The alumina comes more and more contact with sliding surface and results in lowering the frictional coefficients of the composite materials. The worn surfaces of the samples from the SEM examination are shown in Fig 16. The worn surfaces of the (Al-4.2%Cu-3.4% $Al_2O_3$) samples were noticed to be smoother than those of the (Al-4.2%Cu-3.4% $Al_2O_3$). Generally, the parallel ploughing grooves and scratches can be seen over all the surfaces in the direction of sliding. These grooves and scratches resulted from the ploughing action of asperities on the counter disc of significantly higher hardness. The worn surfaces of the samples from the SEM examination are shown in Fig.16 (a & b). The worn surfaces of the test sample were noticed to be smoother at the higher load than at the lower load as shown in Fig 14. Generally, the parallel ploughing grooves and scratches can be seen over all the surfaces in the direction of sliding. These grooves and scratches resulted from the ploughing action of asperities on the counter disc of significantly higher hardness [11-13].

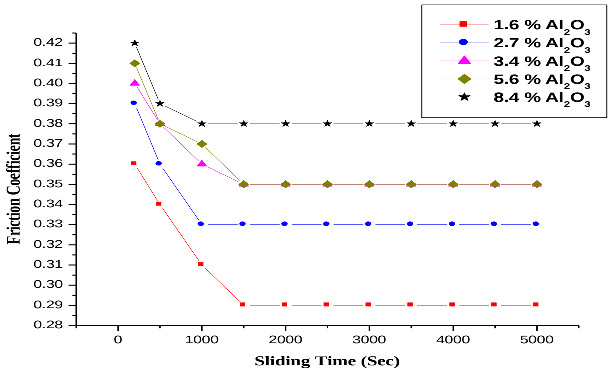


**Fig.13: Friction coefficient variation of Al-Cu/ Alumina composite during sliding time at fixed specific loads (i.e. 10N) and sliding speeds (1.22 m/sec)**

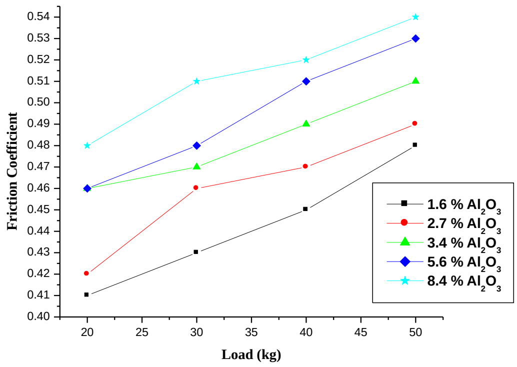


**Fig.14: Coefficient of friction vs. applied load for Al-Cu/ $Al_2O_3$ composite at 0.932m/sec**

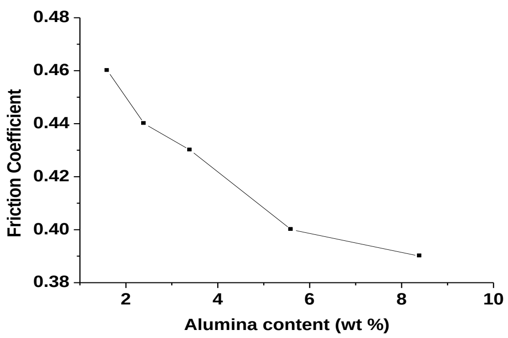


**Fig.15: Variations in the coefficient of friction with the wt % of $Al_2O_3$ in the matrix.**

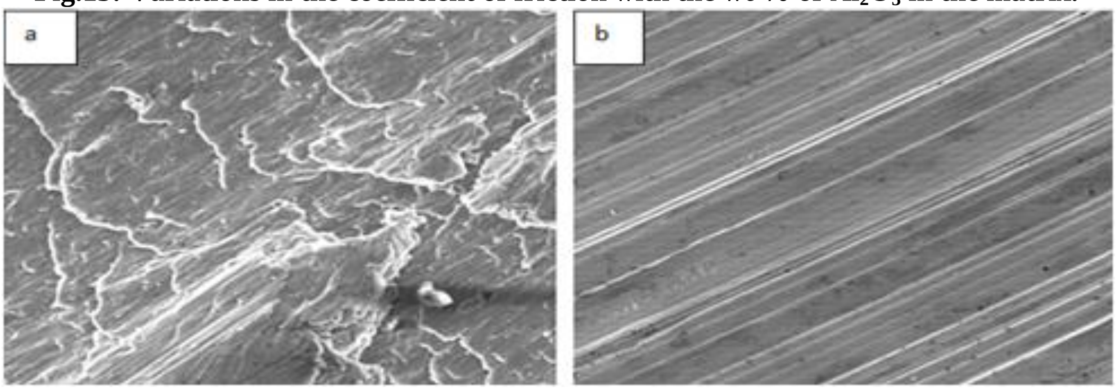


**Fig.16: SEM micrographs of wear debris of (Al-4.2%Cu-3.4% $Al_2O_3$) for 2 kg applied load and 1.22 m/s sliding velocity at 3000 m sliding distances (a) at lower loads (b) at higher loads**

## VIII. Conclusion

1. The Al-Cu/Alumina composite is being prepared from liquid metallurgical methods. It can be observed from the present investigation that alumina could be successfully and uniformly distributed in aluminium-Copper base matrix using impeller mixing chill casting technique.
2. UTS (Ultimate Tensile Strength), 0.2% PS (Proof Stress) and VHN (Vickers Hardness Number) increased with increases the volume fraction of the alumina in the matrix.
3. The Al-4.2% Cu-8.4% $Al_2O_3$ composite showed lower percentage of elongation while compared to Al-4.2%Cu -1.6% $Al_2O_3$ From the present investigation we have also observed that the ductility of composite decreases with increase the percentage of alumina.
4. The hardness is another affecting parameter which affects the rate of wear, increases with decreases the percentage of alumina in the matrix.
5. Wear rate with sliding distance shows almost a linear relationship for all combinations of loads and sliding velocities and composites.
6. Wear rate increases continuously with applied load for all the sliding velocities and composites studied.
7. Low loads and sliding velocities are dominated by oxidative debris whereas higher loads and sliding velocities are dominated by metallic debris.
8. At low loads and sliding velocities wear track surface is largely covered with oxide layer and smooth in nature but at higher loads or sliding velocities surface is highly deformed with deep grooves and gross delaminating occurs leading to larger wear rate.

The coefficient of friction decreases with increase the alumina content in the matrix.

## References:

[1] K.K. Chawla., Composite Materials, 2nd ed., Springer, New York, 1998, p 3–5
[2] T.W. Clyne. and Withers P.J., An Introduction to Metal Matrix Composites, 1st ed., Cambridge University Press, Cambridge, 1993,p 1–10.
[3] B. K. Prasad.: Effects of microstructure on the sliding wear performance of Zn-Al-Ni alloy, Wear 240(2000), 100-112.
[4] G Purcek., T Kucukomeroglu , T. Savaskan., and S. Murphy.: Dry sliding friction and wear properties of zinc-based alloy, Wear 252(2002), 894 – 901,
[5] Sheng-ming Zhou, Xiao-bin Zhang, Zhi-peng Ding, Chun-yan Min, Guo-liang Xu, Wen-ming Zhu. Fabrication and tribological properties of carbon nanotubes reinforced Al composites prepared by pressure less infiltration technique [J]. Composites Part A: Applied Science and Manufacturing, 2007, 38(2): 301−306.
[6] N. P. Suh. The delamination theory of wear [J]. Wear, 1973, 25(1): 111−124.−13
[7] F.Akhlaghi, and A. Zare-Bidaki., Influence of alumina content on the dry sliding and oil impregnated sliding wear behavior of aluminum 2024 – alumina composites produced by in situ powder metallurgy method. Wear 266 (2009) 37-45.
[8] Rohatgi P.K. and Pai B.C., Seizure Resistance of Cast Aluminum Alloys Containing Dispersed Alumina Particles of Various Sizes, Wear, 1980, 59, p 323–332
[9] Prasad S.V. and Asthana R., Aluminum Metal Matrix Composites for Automotive Applications: Tribological Considerations, Tribol. Lett., 2004, 17(3), p 445–453
[10] Gibson P.R., Clegg A. J. and Das A.A., Wear of cast Al-Si alloys containing alumina: Wear, vol 95(1984) 193-198.
[11] Das S., Prasad S.V., Ramachandran T.R., Wear 133 (1989) 173-187.
[12] Lin, C.B., Chang R.J., Weng W.P., A study on process and Tribological behavior of aluminum alloy / Alumina particle composite, Wear 217 (1998) 167-174.
[13] Savaskan T., and Aydiner A. Effects of silicon content on the mechanical and tribological properties of monotectoid-based zinc-silicon-silicon alloys, Wear 257(2004), 377-388,.
[14] H.J. Lee, H. Yamauchi, H. Suda, K. Haraya, Sep. Purif. Technol. 49 (2006) 49